Taylor & Francis
Taylor & Francis Group

Natural Product Research
Formerly Natural Product Letters

ISSN: 1478-6419 (Print) 1478-6427 (Online) Journal homepage: https://www.tandfonline.com/loi/gnpl20

Three new cycloart-7-ene triterpenoid glycosides from *Cimicifuga dahurica* and their anti-inflammatory effects

Qian-Qian Pang, Yu-Dan Mei, Yuan-Chu Zhang, Ling-Xian Liu, Dan-Feng Shi, Da-Bo Pan, Xin-Sheng Yao, Hai-Bo Li & Yang Yu

To cite this article: Qian-Qian Pang, Yu-Dan Mei, Yuan-Chu Zhang, Ling-Xian Liu, Dan-Feng Shi, Da-Bo Pan, Xin-Sheng Yao, Hai-Bo Li & Yang Yu (2020): Three new cycloart-7-ene triterpenoid glycosides from *Cimicifuga dahurica* and their anti-inflammatory effects, Natural Product Research, DOI: 10.1080/14786419.2020.1719487

To link to this article: https://doi.org/10.1080/14786419.2020.1719487

NATURAL PRODUCT RESEARCH
https://doi.org/10.1080/14786419.2020.1719487

Three new cycloart-7-ene triterpenoid glycosides from *Cimicifuga dahurica* and their anti-inflammatory effects

Qian-Qian Pang[a]*, Yu-Dan Mei[b]*, Yuan-Chu Zhang[a], Ling-Xian Liu[a], Dan-Feng Shi[a], Da-Bo Pan[a], Xin-Sheng Yao[a], Hai-Bo Li[b] and Yang Yu[a]

[a]Institute of Traditional Chinese Medicine & Natural Products, College of Pharmacy and Guangdong Province Key Laboratory of Pharmacodynamic Constituents of TCM and New Drugs Research, Jinan University, Guangzhou, People's Republic of China; [b]State Key Laboratory of New-tech for Chinese Medicine Pharmaceutical Process, Jiangsu Kanion Pharmaceutical Co. Ltd, Jiangsu, Lianyungang, People's Republic of China

ABSTRACT

Ten cycloart-7-ene triterpenoid glycosides, including three new compounds (**1**–**3**), were isolated from the roots of *Cimicifuga dahurica*. Their structures were elucidated on the basis of extensive spectroscopic analyses, chemical methods and comparison with literatures. In addition, the isolates were evaluated for their inhibitory effects on the production of NO, as well as the expressions of iNOS and COX-2 in LPS-stimulated RAW 264.7 macrophages. The results showed that compounds **3**, **5**, **6**, **7** and **8** can reduce the release of NO in a dose-dependent manner. Mechanistically, Western blot analysis indicated that the NO inhibitory effects relied on down-regulating the expression of iNOS, and partially associated with lowering the expression of COX-2.

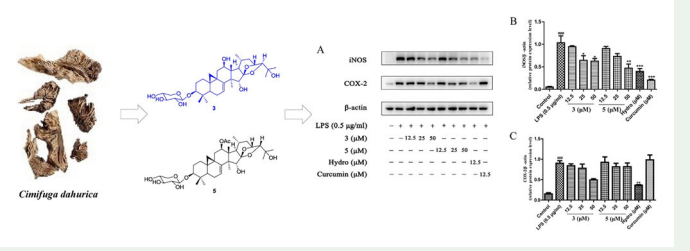

ARTICLE HISTORY
Received 7 November 2019
Accepted 11 January 2020

KEYWORDS
Cimicifuga dahurica; cycloart-7-ene triterpenoid glycosides; anti-inflammatory; NO; iNOS; COX-2

1. Introduction

The genus *Cimicifuga* plants, belonging to the family Ranunculaceae, have an extensive history of use in China, Japan, Europe and North America (Guo et al. 2017). Cimicifuga Rhizome, originated from *C. heracleifolia* Kom., *Cimicifuga dahurica* (Turcz.) Maxim. and *C. foetida* L., is officially listed in *Chinese Pharmacopeia* (Commission NP

CONTACT Yang Yu 1018yuyang@jnu.edu.cn; Hai-Bo Li lihaibo1985124@sina.com
*The first two authors contributed equally to this work.
Supplemental data for this article can be accessed at https://doi.org/10.1080/14786419.2020.1719487.

2015) for the treatment of headache, toothache, aphtha, sore throat and uterine prolapse. Previous phytochemical studies have revealed that it mainly contained 9,19-cycloartane triterpenes (Liu et al. 2003; Sun et al. 2016; Hao et al. 2019), cinnamic acids (Qin et al. 2016), chromones (Shi et al. 2018) and nitrogenous compounds (Zhang et al. 2013). More strikingly, cycloartane triterpenes have been reported to be the major characteristic components in *Cimicifuga* showing diverse bioactivities, including anti-tumour (Liu et al. 2014; Sun et al. 2017), neuro-protection (Lv et al. 2017), anti-inflammation (Thao et al. 2018) and so on (Su et al. 2016).

Natural compounds in medical plants are always found to play an important role in inflammatory disease (Maione et al. 2016). In our research for anti-inflamatory agents from *Cimicifuga* plants, an investigation of *C. dahurica* resulted in the isolation of new bioactive phenolic acids (Lu et al. 2019a, 2019b). As a continuing effort to enrich and deeply investigate the potent anti-inflamatory agents, ten cycloart-7-ene triterpenoid glycosides, including three new triterpenes (**1**–**3**), were obtained from the extract of *C. dahurica*. Their structures were unambiguously elucidated by analysing spectroscopic data, using chemical methods, or comparing their NMR data with those in the literatures. In addition, we examined the *in vitro* effects of the isolates on the production of nitric oxide (NO), as well as the expressions of inducible NO synthase (iNOS) and cyclooxygenase-2 (COX-2) in LPS-stimulated RAW 264.7 cells.

2. Results and discussion

2.1. Structure determination

Compound **1** was isolated as a white amorphous powder, m.p. 190–195 °C, [α]25 D −23.4. Its molecular formula was established as $C_{35}H_{54}O_{10}$ based on the HRESIMS data (*m/z* 657.3605 $[M + Na]^+$, calcd. for $C_{35}H_{54}O_{10}Na$, 657.3615), accounting for nine degrees of unsaturation. The ^1H NMR spectrum (600 MHz, in pyridine-d_5) of **1** showed typical signals due to a cyclopropane methylene [δ_H 1.12, 0.55, each, *d*, $J = 4.0$ Hz, H_2-19], seven tertiary methyls [δ_H 1.78 (H_3-21), 1.59 (H_3-18), 1.54 (H_3-27), 1.48 (H_3-26), 1.39 (H_3-28), 1.38 (H_3-29), 1.11 (H_3-30)], an olefin [δ_H 6.18, dd, $J = 7.6$, 2.0 Hz, H-7] and an anomeric proton [δ_H 4.89 (1 H, d, $J = 7.5$ Hz, H-1′)], indicating a cycloartane-type triterpenoid glycoside. The ^{13}C NMR (150 MHz, in pyridine-d_5) and DEPT 135 spectra of **1** displayed a total of 35 carbon signals. Except for five glycosyl carbons, the remaining 30 aglycone carbons were resolved as 9 quaternary carbons (a carbonyl group), 7 methines (an olefinic, and 5 oxygenated), 7 methylenes and 7 methyls. In addition, an NMR comparison analysis with a known compound (Nishida and Yoshimitsu 2011), allowed the establishment of a cycloart-7-en rings A–D in **1**. This conclusion can be supported by three spin systems (H_2-1/H_2-2/H-3, H-5/H_2-6/H-7 and H_2-11/H_2-12) in ^1H–^1H COSY, as well as key correlations of H_3-29(30)/C-3, 4, 5; H_2-19/C-1, 9, 10, 11; H_3-18/C-12, 13, 14, 17; H_3-28/C-8, 13, 14, 15 and H-15, 17/C-16 (supplementary material Figure S1) in HMBC spectrum. Meanwhile, the COSY correlations of H_2-22/H-23/H-24, together with HMBC correlations of H_3-21/C-17, 20, 22, H_3-26(27)/C-24, 25 and H-24/C-20, led to the establishment of a five-membered side chain (ring E) with the C20, 24-ether linkage (supplementary material Figure S1). The hydrolysis of compound **1** offered a D-xylose, which was determined by derivatisation and HPLC analysis (Tanaka et al. 2007). A β-D-xylose was deduced

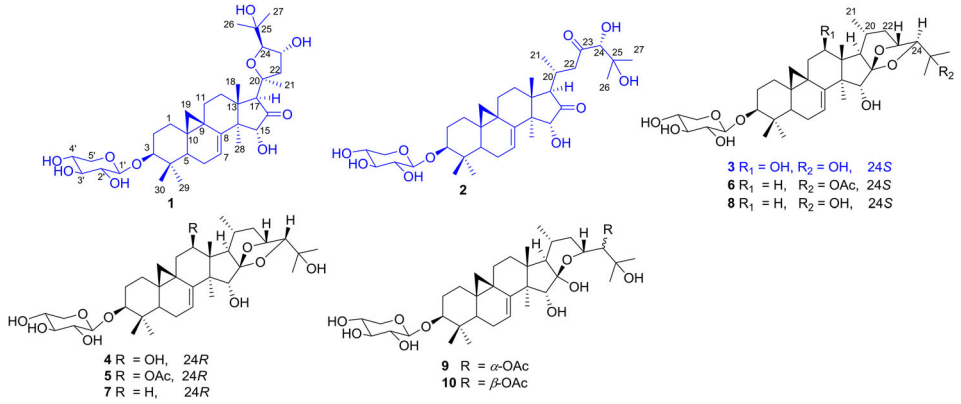

Figure 1. Structures of compounds **1–10**.

due to the *J* value ($J_{1',\ 2'}$=7.5 Hz). The sugar unit was confirmed to attached to C-3 by the HMBC correlation peaks of H-1′ (δ_H 4.89)/C-3(δ_C 88.3), and H-3 (δ_H 3.54)/C-1′(107.6). Thus, the planar structure of **1** was established.

The relative stereochemistry of **1** was disclosed by coupling constants and the ROESY experiment. The large coupling constants of H-3 (δ_H 3.54, dd, J = 11.6, 4.1 Hz) supported the assignment of 3β-OH. Moreover, ROESY correlations of H_3-29/H-3/H-5, H_3-30/H_2-19/H_3-18/H-15 and H_3-28/H-17, indicated that A/B, C/D rings were *trans*-fused, and H-17 and 15-OH were α-oriented (supplementary material Figure S1). In addition, based on a reported method of computational chemistry (Gan et al. 2015), the free rotation of the C-17-C-20 single bond was considered to be restricted to some extent in 20,24-epoxy-cycloartane triterpenoids. The H-24α and H-23β were assigned by key correlations of H-17/H_3-21, H_3-21/H-24 and H-23/H_3-26(27) observed in ROESY spectrum (supplementary material Figure S1). Hence, compound **1** was elucidated as (20*S*,24*R*)-20,24-epoxy-15α,23β,25-trihydroxy-3β-(β-D-xylopyranosyloxy)-9,19-cycloart-7-en-16-one (Figure 1).

Compound **2** was isolated as a colourless amorphous powder, m.p. 295–301 °C, [α]25 D –52.4 and its molecular formula $C_{35}H_{54}O_{10}$ was determined by HRESIMS data (*m/z* 657.3620, $[M + Na]^+$, calcd. for $C_{35}H_{54}O_{10}Na$, 657.3615), implying nine degrees of unsaturation. The ^{13}C NMR spectrum of **2** was similar to those of **1** except C-17 side chain moiety (Table S1). With the aid of 2 D NMR spectra, A–D rings of cyclopropane structure in **2** were assigned as the same as **1** (supplementary material Figure S2). Besides, a sequence connected through the correlations of H-17/H-20(H_3-21)/H_2-22 in the ^1H–^1H COSY, combined with the long-range correlations of H_2-22/C-23, H-24/C-23, 25, H_3-26(27)/C-24, 25, led to a C20–C27 side chain. Therefore, the structure of **2** was established as an 11-dehydroxylated derivative of 15α-hydroxyximicidol-3-*O*-β-D-xylopyranoside (Kadota et al. 1995). By comparing their NMR data, it could be deduced that **2** possessed the same stereochemistry with this known compound, which was further confirmed by the ROESY experiment (supplementary material Figure S2). Except for C-24, the other chiral centres in compound **2** were consistent with **1** for ROESY correlations of H-3/H_3-29, H_2-19/H_3-18(H-20)/H-15 and H_3-28/H-17/H_3-21. Further, 24α-OH was determined by ROESY correlations of H_3-21/H-22α (δ_H 3.24) and

H-22β (δ_H 4.22)/H-24. As a result, compound **2** was established and named 11-dehydro-15α-hydroxyximicidol-3-*O*-β-D-xylopyranoside (Figure 1).

Compound **3** was obtained as a white amorphous powder, m.p. 266–270 °C, [α]25 D −37.6, and a molecular formula determined to be $C_{35}H_{54}O_{10}$ on the basis of HRESIMS data (*m/z* 635.3795, $[M+H]^+$, calcd. for $C_{35}H_{55}O_{10}$, 635.3795). Compound **3** possessed the same aglycone as bugbanoside F and 7,8-didehydro-12-β-hydroxyl-cimigenol-3-*O*-β-D-galactopyranoside for their similar NMR data (supplementary material Table S1), which can be supported by the detailed analysis of key ^{1}H–^{1}H COSY and HMBC correlations (supplementary material Figure S3). Similarly, the sugar unit in **3** was determined as a β-D-xylose by the same method as compound **1**. For the stereochemistry of **3**, the large coupling constants of H-3 (δ_H 3.49, dd, $J = 11.6$, 4.1 Hz) and H-12 (δ_H 4.36, dd, $J = 11.3$, 5.2 Hz) were observed in ^{1}H NMR spectrum. Observed ROESY correlations were H-5/H-3/H_3-29, H_3-30/H_2-19/H_3-18/12-OH, H-15/H_3-18/H-20, H_3-28/H-17/H_3-21, H-23/H_3-26(27) and H-24/H-17, indicating the existence of 3β-OH, 12β-OH, 15α-OH, H-17α, H-23α and H-24β (supplementary material Figure S3). Furthermore, as concluded from those 24-configuration triterpenes (Li et al. 1993), the absolute configuration of C-24 in **3** can be assigned as 24*S* for a single or broad single peak ($J < 1.0$ Hz) (whereas a double peak, $J \approx 4.0$ Hz for 24*R*). Thereafter, compound **3** was established as 12β-hydroxy-7,8-didehydrocimigenol-3-*O*-β-D-xylopyranoside (Figure 1).

The seven known compounds (**4**–**10**) were identified as (23*R*,24*R*)-16β,23;16α,24-diepoxy-cycloart-7-en-3β,12β,15α,25-tetraol-3-*O*-β-D-xylopyranoside (**4**) (Yoshimitsu et al. 2006), (23*R*,24*R*)-16β,23;16α,24-diepoxy-12β-acetoxy-cycloart-7-en-3β,15α,25-triol-3-*O*-β-D-xylopyranoside (**5**) (Yoshimitsu et al. 2006), 25-*O*-acetyl-7,8-didehydrocimigenol-3-*O*-β-D-xylopyaranoside (**6**) (Kusano et al. 1999), 24-*epi*-7,8-didehydrocimigenol-3-*O*-β-D-xylopyaranoside (**7**) (Li et al. 1993), 7,8-didehydrocimigenol-3-*O*-β-D-xylopyaranoside (**8**) (Kusano et al. 1999), 24-*O*-acetyl-7,8-didehydro-hydroshengmanol 3-*O*-β-D-xylopyranoside (**9**) (Kusano et al. 1999) 24-*epi*-24-*O*-acetyl-7,8-didehydro-hydroshengmanol-3-*O*-β-D-xylopyranoside (**10**) (Kusano et al. 1999), respectively, by comparison of their spectroscopic data with those reported in the literatures.

2.2. Anti-inflammatory activities

For evaluating the anti-inflammatory effects, compounds were assayed on NO production in LPS-stimulated RAW264.7 cells. As shown in supplementary material Figure S6, the NO production in the model groups (simulated with LPS) increased significantly, whereas the production of NO decreased in the treatment groups as compared with that in model cells. The results suggested that compounds inhibited the release of NO in a dose-dependent manner. In conclusion, some of the isolates can significantly inhibit NO-production during LPS-stimulated inflammatory response.

In order to further illuminate the anti-inflammatory effects, compounds **3** and **5** were selected as examples to test the impact on protein levels of iNOS and COX-2 by Western blot. As shown in supplementary material Figure S7, the expressions of iNOS and COX-2 in non-treated cells simulated with LPS was significantly increased compared with the control groups. The decreases of iNOS protein in the treatment groups

were consistent with the trends of NO production, whereas the protein level of COX-2 did not noticeably decrease. The results of Western blot analysis indicated that the anti-inflammatory effects of **3** and **5** mainly relied on down-regulating the expression of iNOS, and partially associated with lowering the expression of COX-2.

The cytotoxicity of the tested compounds was evaluated in the presence or absence of LPS by MTT assay as reported previously (Mei et al. 2019). All the tested compounds did not decrease the viability of RAW264.7 cells when they were incubated with or without LPS (0.5 μg/mL) at the test concentration (data were present in supplementary material Figure S4 and S5).

3. Experimental

3.1. Instrumentations and reagents

Melting points were determined on an X-5 micromelting point apparatus (Beijing TECH Instrument Co. Ltd, Beijing, China) and are reported uncorrected. Optical rotations were measured on a JASCO P-1020 polarimeter with a 1-cm cell at room temperature. IR spectra were recorded in KBr disc with a JASCO FT/IR-480 Plus. NMR spectra were recorded on a Bruker Avance 600 spectrometer (Bruker Co. Ltd., Bremen, Germany) in pyridine-d_5 (CIL, USA). HRESIMS spectra were performed on a Waters Synapt G2 Q-TOF (Waters, Manchester, UK) with a Waters RP-18 column (Acquity BEH, 1.7 m, ϕ 3.0 × 150 mm). HPLC analyses were performed on a Shimadzu LC-20AB (or Waters 2695) coupled with a Phenomenex Gemini C18 column (5 μm, ϕ 4.6 × 250 mm; FLM Inc., Guangzhou, China), while preparative HPLC was performed on an LC-20AB (or Waters 1515) using a Phenomenex Gemini C18 column (5 μm, ϕ 10 × 250 mm; FLM Inc., Guangzhou, China). Column chromatography (CC) was carried out over Diaion HP-20 (Mitsubishi Chemical Co.), silica gel (200–300 mesh, Qingdao Marine Chemical Ltd.), ODS-silica gel (12 nm, S-50 μm, YMC Ltd.), Sephadex LH-20 (Amersham Pharmacia Biotech), pre-coated silica gel plate (SGF_{254}, 0.2 mm, Yantai Chemical Industry Research Institute).

The methanol and acetonitrile of HPLC grade (Merck, Shanghai, China) were used in HPLC. L-Cysteine methyl ester hydrochloride, *o*-tolyl isothiocyanate and the standard monosaccharides were purchased from Aladdin Reagent CO., Ltd., Shanghai, China, while the other solvents were purchased from Baishi Chemical Industry CO., Ltd., Tianjin, China.

3.2. Plant material

The roots of *C. dahurica* were collected in Heilongjiang Province, China, in June 2015, and were identified by Prof. Haixue Kuang (Heilongjiang University of Chinese Medicine). A sample (JNUCD201506) was deposited in Institute of Traditional Chinese Medicine & Natural Products, college of pharmacy, Jinan University, Guangzhou, China.

3.3. Extraction and isolation

Air-dried rhizomes of *C. dahurica* (19.5 kg) were pulverised and extracted three times with 60% EtOH under reflux conditions. The 60% EtOH extract was concentrated under reduced pressure, yielding a viscous residue (3.6 kg), which was subjected to HP-20

macroporous adsorption resin CC to yield H_2O fraction, 30% ethanol fraction (384 g) and 95% ethanol fraction (534 g). The 95% ethanol fraction (450 g) was subjected to silica gel CC using a stepwise gradient elution of CH_2Cl_2–CH_3OH (100:0, 99:1, 98:2, 97:3, 95:5, 90:10, 80:20, 70:30, 60:40, 0:100) to afford 12 subfractions (A–L). Fraction G (40 g) was chromatographed over an ODS CC using CH_3OH–H_2O as eluent (30:70, 50:50, 70:30, v/v) to give 7 subfractions (G1–G7). Fraction G4 (7.0 g) was further separated on a silica gel column eluted with CH_2Cl_2–CH_3OH (100:1 to 0:100, v/v), affording subfractions G4A–G4E. By using semi-preparative HPLC, subfraction G4B was purified with CH_3CN–H_2O (35:65) to give **3** (13.8 mg) and **8** [160 mg, [α]25D −15.3 (*c* 1.0, MeOH)], while G4C offer **1** (5.2 mg) and **2** (180 mg) with CH_3CN–H_2O (30:67). Fraction G5 (21 g) was further separated into five subfractions G5A–G5G on a silica gel CC by using CH_2Cl_2–CH_3OH gradiently (100:1 to 0:100, v/v). Then subfraction G5C was purified by Sephadex LH-20 (CH_3OH) and semi-preparative HPLC with CH_3CN–H_2O (40:60), giving **4** [15.3 mg, [α]25D −22.3 (*c* 1.0, MeOH)], **5** [113 mg, [α]25D −28.5 (*c* 1.0, MeOH)], **6** [46 mg, [α]25D −15.5 (*c* 1.0, MeOH)], and **9** [14.3 mg, [α]25 D–46.4 (*c* 1.0, MeOH)]. Subfraction G5D was purified by using semi-preparative HPLC with CH_3CN–H_2O (45:55) to yield **7** [53 mg, [α]25D −13.7 (*c* 1.0, MeOH)] and **10** [67 mg, [α]25D −26.4 (*c* 1.0, MeOH)].

3.4. Spectroscopic data of compounds 1–3

(20*S,24*R)-20,24-epoxy-15α,23β,25-trihydroxy-3β-(β-D-xylopyranosyloxy)-9,19-cycloart-7-en-16-one **(1).** Colourless amorphous powder; m.p. 190–195 °C, [α]25D −23.4 (*c* 0.5, MeOH); IR (KBr) ν_{max}: 3409, 2967, 2937, 2872, 1737, 1457, 1382, 1069, 1046 cm^{-1}; ^1H NMR (pyridine-d_5, 600 MHz) and ^{13}C NMR (*pyridine*-d_5, 150 MHz) data, seen supplementary material Table S1 and Figures S9–S17; HR ESI MS: *m/z* 657.3605 $[M + Na]^+$ (calcd. for $C_{35}H_{55}O_{10}$, 657.3615).

11-dehydro-15α-hydroxyximicidol-3-O-β-D-xylopyranoside **(2)**. White amorphous powder; IR(KBr) ν_{max} 3397, 2969, 2935, 2872, 1735, 1700, 1465, 1383, 1078, 1039 cm^{-1}; m.p. 295–301 °C, [α]25D −52.4 (*c* 1.0, MeOH); ^1H NMR (pyridine-d_5, 600 MHz) and ^{13}C NMR (*pyridine*-d_5, 150 MHz) data, seen supplementary material Table S1 and Figures S18–S26; HR ESI MS: *m/z* 657.3620 $[M + Na]^+$ ($C_{35}H_{55}O_{10}$, calcd. 657.3615).

12β-hydroxy-7,8-didehydrocimigenol-3-O-β-D-xylopyranoside **(3).** White amorphous powder; IR(KBr) ν_{max} 3452, 2976, 2950, 1169, 1066, 1032 cm^{-1}; m.p. 266–270 °C, [α]25D −37.6 (*c* 1.0, MeOH); ^1H NMR (pyridine-d_5, 600 MHz) and ^{13}C NMR (*pyridine*-d_5, 150 MHz) data, seen supplementary material Table S1 and Figures S27–S35; HR ESI MS: *m/z* 635.3795 $[M + H]^+$(calcd. for $C_{35}H_{55}O_{10}$, 635.3795).

3.5. Acid hydrolysis of compounds 1–3

The acid hydrolysis of compounds **1**–**3** was performed as the literature (Tanaka et al. 2007). A solution of each compound (1.0 mg) was hydrolysed in 2 mL HCl (2 mol/L) under 80–90 °C for 1 h. The reaction mixture was partitioned between EtOAc and H_2O twice. The H_2O layer was concentrated under reduced pressure, giving a saccharide residue. The residue was dissolved in pyridine (1.0 mL) containing L-cysteine methyl

ester hydrochloride (2.5 mg) and heated at 60 °C. 1 h later, *o*-tolyl isothiocyanate (10 μL) was added and further reacted at 60 °C for 1 h. Then, the reaction mixture was directly analysed by the HPLC system and detected with a UV detector at the wavelength of 250 nm on a C18 column at 35 °C. The mobile phase was $CH_3CN - H_2O - HCOOH$ (25:75:0.1, v/v/v) at a flow rate of 0.8 mL/min. The standard monosaccharides, D-xylose and L-xylose, were subjected to the same method. As a result, the monosaccharides of **1**–**3** were determined to be D-xylose by comparing retention time with derivatisation of standard monosaccharides in HPLC chromatogram (supplementary material Figure S8).

3.6. Anti-inflammation activity assay

The assay was carried out as previously described (Zhao et al. 2012) with minor modifications.

3.6.1. Cell cultures

Mouse RAW264.7 macrophage cells were obtained from ATCC and cultured in Dullbecco's modified Eage's medium (DMEM) containing 10% foetal bovine serum (Gibco: C11995500BT), 100 U/mL penicillin and 100 μg/mL streptomycin (Gibco:15140-122) with 5% CO_2 at 37 °C.

3.6.2. Measurement of cell viability

The viability of mouse RAW264.7 macrophage cells was determined by MTT (Methylcyclopentadienyl Manganese Tricarbonyl, Aladdin: T100896-5g). The RAW264.7 cells were seeded into 96-well plate (Nest, Biotech, China) with a density of 2.5×10^4 cells/mL. After treatment with series concentrations of compounds for 24 h, the absorbance (490 nm) was recorded on a microplate reader (BioTek Instruments: SN258282).

3.6.3. Bioassay for NO production

Nitrite, as an indicator of NO production, was measured for its concentration in medium according to Griess method (Beyotime Biotechnology, S0021). Hydrocortisone (Aladdin: C1710078) and curcumin (Meilunbio: N0223A) were used as positive controls. RAW264.7 cells were seeded into 96-well plates at 2.5×10^4 cells/well and cultured overnight. Subsequently, the cells were incubated in new medium which included 0.5 μg/mL LPS with or without the compounds for additional 24 h at 37 °C. The cell-free supernatant and Griess reagents (Griess Reagent I and Griess Reagent II) were completely mixed with the same amount of 50 μL. Absorbance of the final product was measured at 540 nm on the microplate reader. The nitrite concentration and inhibitory rate were calculated according to the standard calibration curve. The residual cell-free supernatant was removed and added 100 μL fresh DMEM, and then the viability of the RAW264.7 cells was determined by MTT.

3.6.4. Western blot assay

Western blot analysis was performed to evaluate the expression of inflammation-associated proteins, such as iNOS and COX-2 proteins. Cells were collected, then

resuspended with radio immunoprecipitation assay buffer (Fdbio: FD008) supplemented with 0.1 mM PMSF protease inhibitor (Fdbio: FD1001). The cell suspension was vortexed and lysed by ultrasound and then centrifuged at 12,000 rpm, then the supernatant was taken and reserved. The total protein concentrations were determined by BCA protein assay kit (Beytime: P0010). The same amount of proteins for each sample was loaded to 8% sodium dodecyl sulphate polyacrylamide gel electrophoresis (SDS-PAGE), and the proteins separated on the gel were transferred onto a polyvinylidene difluoride membrane (Immobilon: IPVH00010). After blocking with 5% skim milk (BD: 232100), the membranes were then incubated with specific primary antibodies (iNOS: CST13120s; COX-2: 12282S) at 4 °C overnight, followed by incubation with corresponding secondary antibodies (Fdbio: FDR007). The protein blots were finally detected by enhanced chemiluminsecence system (ImmunoCruz: sc-2048).

3.6.5. Statistical analysis

At least triplicate experiments were conducted to obtain all results, and the data were displayed as mean ± SEM. Statistical analysis was performed on GraphPad, version 4.00, One-way ANOVA followed by Tukey's test were used in the statistical teats. A value of $p < 0.05$ was considered statistically significant.

4. Conclusions

In this study, ten cycloart-7-ene triterpenoid glycosides, including three new compounds (**1**–**3**), were isolated from the roots of *C. dahurica* (Figure 1). Their structures were elucidated on the basis of extensive spectroscopic analyses, chemical methods and comparison with literatures. In addition, the isolates were evaluated for their inhibitory effects on the production of NO, as well as the expressions of iNOS and COX-2 in LPS-stimulated RAW 264.7 macrophages.

Acknowledgement

The authors are grateful to State Key Laboratory of New-Tech for Chinese Medicine Pharmaceutical Process, Jiangsu Kanion Pharmaceutical Co. Ltd. for their assistance of activity test.

Disclosure statement

No potential conflict of interest was reported by the authors.

Funding

This study was supported by grants from the National Natural Science Foundation of China (Grant Nos. 81630097, 81602984, 81803347 and 81903426).

References

Commission NP. 2015. The pharmacopeia of the People's Republic of China. Beijing: China Medical Science Press, 1, p. 73–74.

Gan LS, Zheng DJ, Liu Q, Zhou J, Zhang MZ, Yao W, Shao BH, Mo JX, Zhou CX. 2015. Eight new cycloartane triterpenoids from *Beesia calthifolia* with hepatoprotective effects against D-galactosamine induced L02 cell damage. Bioorg Med Chem Lett. 25(18):3845–3849.

Guo Y, Yin T, Wang X, Zhang F, Pan G, Lv H, Wang X, Owoicho Orgah J, Zhu Y, Wu H. 2017. Traditional uses, phytochemistry, pharmacology and toxicology of the genus *Cimicifuga*: a review. J Ethnopharmacol. 209(1):264–282.

Hao YM, Luo W, Jiang GZ, Lv CN, Lu JC. 2019. One new and seven known triterpene glycosides from the aerial parts of *Cimicifuga dahurica*. J Asian Nat Prod Res. 10.1080/10286020.2019.1638370

Kadota S, Li JX, Tanaka K, Namba T. 1995. Constituents of Cimicifugae Rhizoma. II. Isolation and structures of new cycloartenol triterpenoids and related compounds from *Cimicifuga foetida* L. Tetrahedron. 51(4):1143–1166.

Kusano A, Takahira M, Shibano M, Miyase T, Kusano G. 1999. Studies on the constituents of *Cimicifuga* Species. XXVI. Twelve new cycloart-7-enol glycosides from the underground parts of *Cimicifuga simplex* WORMSK. Chem Pharm Bull. 47(4):511–516.

Li JX, Kadota S, Hattori M, Yoshimachi S, Shiro M, Oogami N, Mizuno H, Namba T. 1993. Constituents of Cimicifugae Rhizoma. I. Isolation and characterization of ten new cycloartenol triterpenes from *Cmicifuga heracleifolia* KOMAROV. Chem Pharm Bull. 41(5):832–841.

Liu DL, Li YJ, Yao N, Xu J, Chen ZS, Yiu A, Zhang CX, Ye WC, Zhang DM. 2014. Acerinol, a cyclolanstane triterpenoid from *Cimicifuga acerina*, reverses ABCB1-mediated multidrug resistance in HepG2/ADM and MCF-7/ADR cells. Eur J Pharmacol. 733:34–44.

Liu Y, Chen D, Si J, Tu G, An D. 2003. Cimidahuside 1 and 2, two new cyclolanostanol xylosides from the aerial parts of *Cimicifuga dahurica*. Nat Prod Res. 17(4):243–246.

Lu Q, Li HB, Pang QQ, Zhang WY, Su ZZ, Pan DB, Yao XS, Yu Y. 2019. New phenylpropanoid allopyranosides from the rhizomes of *Cimicifuga dahurica*. Bioorg Med Chem Lett. 29(14):1774–1778.

Lu Q, Zhang WY, Pan DB, Shi DF, Pang QQ, Li HB, Yao XJ, Yao ZH, Yu Y, Yao XS. 2019. Phenolic acids and their glycosides from the rhizomes of *Cimicifuga dahurica*. Fitoterapia. 134:485–492.

Lv C, Yang F, Qin R, Qi Z, Zhou W, Lu J. 2017. Bioactivity-guided isolation of chemical constituents against H_2O_2-induced neurotoxicity on PC12 from *Cimicifuga dahurica* (Turcz.) Maxim. Bioorg Med Chem Lett. 27(15):3305–3309.

Maione F, Russo R, Khan H, Mascolo N. 2016. Medicinal plants with anti-inflammatory activities. Nat Prod Res. 30(12):1343–1352.

Mei YD, Zhang N, Zhang WY, Tang JS, Zhou H, Yu Y, Yao XS. 2019. Two new ursane-type nortriterpenes from *Lonicera macranthoides* and their iNOS-inhibitory activities. Chin J Nat Med. 17(1):27–32.

Nishida M, Yoshimitsu H. 2011. Six new cycloartane glycosides from Cimicifuga Rhizome. Chem Pharm Bull. 59(10):1243–1249.

Qin R, Zhao Y, Zhao Y, Zhou W, Lv C, Lu J. 2016. Polyphenolic compounds with antioxidant potential and neuro-protective effect from *Cimicifuga dahurica* (Turcz.) Maxim. Fitoterapia. 115:52–56.

Shi QQ, Lu J, Peng XR, Li DS, Zhou L, Qiu MH. 2018. Cimitriteromone A-G, macromolecular triterpenoid-chromone hybrids from the Rhizomes of *Cimicifuga foetida*. J Org Chem. 83(17):10359–10369.

Su Y, Chi WC, Wu L, Wang QH, Kuang HX. 2016. Photochemistry and pharmacology of 9,19-cyclolanostane glycosides isolated from genus *Cimicifuga*. Chin J Nat Med. 14(10):721–731.

Sun HY, Huang MH, Yao N, Hu JY, Li YI, Chen LP, Hu N, Ye WC, Tai WCS, Zhang DM et al. 2017. The cycloartane triterpenoid ADCX impairs autophagic degradation through Akt overactivation and promotes apoptotic cell death in multidrug-resistant HepG2/ADM cells. Biochem Pharmacol. 146:87–100.

Sun HY, Liu BB, Hu JY, Xu LJ, Chan SW, Chan CO, Mok DKW, Zhang DM, Ye WC, Chen SB. 2016. Novel cycloartane triterpenoid from *Cimicifuga foetida* (Sheng ma) induces mitochondrial apoptosis via inhibiting Raf/MEK/ERK pathway and Akt phosphorylation in human breast carcinoma MCF-7 cells. Chin Med. 11:1

Tanaka T, Nakashima T, Ueda T, Tomii K, Kouno I. 2007. Facile discrimination of aldose enantiomers by reversed-phase HPLC. Chem Pharm Bull. 55(6):899–901.

Thao NP, Lee YS, Luyen BTT, Oanh HV, Ali I, Arooj M, Koh YS, Yang SY, Kim YH. 2018. Chemicals from *Cimicifuga dahurica* and their inhibitory effects on pro-inflammatory cytokine production by LPS-stimulated bone marrow-derived dendritic cells. Nat Prod Sci. 24(3):194.

Yoshimitsu H, Nishida M, Sakaguchi M, Nohara T. 2006. Two new 15-deoxycimigenol-type and three new 24-epi-cimigenol-type glycosides from Cimicifuga Rhizome. Chem Pharm Bull. 54(9):1322–1325.

Zhang F, Han LF, Pan G-X, Peng S, Andre N. 2013. A new phenolic amide glycoside from *Cimicifuga dahurica*. Yao Xue Xue Baol. 48(8):1281–1285.

Zhao F, Gao Z, Jiao W, Chen L, Chen L, Yao X. 2012. In vitro anti-inflammatory effects of beta-carboline alkaloids, isolated from *Picrasma quassioides*, through inhibition of the iNOS pathway. Planta Med. 78(18):1906–1911.